Adaptive Linear Prediction Based Buried Object Detection with Varying Detector Height

Ahmet Burak Yoldemir and Mehmet Sezgin
TÜBİTAK UEKAE
Gebze, Kocaeli, TURKEY

***Abstract*—In the GPR underground inspection problem, received GPR signal is notably dependent on the height of the detector head. A great deal of the former research in this area assumes constant detector height, as absence of this constancy will result in undesired change in the returning signal, which will reduce the success of the detection and identification stages. In this study, we propose a buried object detection method which removes the deforming effect of the variable sensor height. In our approach, adaptive one-sided linear prediction is utilized in a specific manner. The proposed algorithm is causal, which makes it convenient for real time buried object detection applications.**

***Index Terms*—Buried object detection, ground penetrating radar, adaptive linear prediction, spatial domain.**

I. Introduction

Underground inspection using ground penetrating radar (GPR) has a wide spectrum of application areas, some of which are mapping of buried archaeological sites [1]–[3], detection of tree defects [4], road evaluation [5], sedimentology [6], evaluation of underground infrastructure [7] and estimation of soil moisture content [8]. GPR is a noninvasive tool which operates by locating the electrical discontinuities in the subsurface. It has been found to be very promising to render the ground and its contents among many other methods, some of which rely on induced polarization, gravity surveying, magnetic surveying, radiometry and thermography [9].

Received GPR signal, however, requires a great deal of processing before it can be utilized. Extensive research was carried out on this topic and many well-known signal processing techniques were applied to received GPR signal. In [10], a gradient method was proposed to identify the hyperbolic shapes produced by land mines for detection, combined with fuzzy logic fusion to further improve the detection accuracy. In another study, hidden Markov models are trained on object and clutter signatures to compute the likelihood that signal returns are due to buried objects [11]. A change detection method based on a sequential probability ratio test is introduced in [12]. In [13], principal component analysis (PCA) is used to differentiate the object and clutter signatures inherent in the GPR data, and the method is further improved by template matching. In a following study, independent component analysis (ICA) is used to detect changes in the GPR data, and the results are compared with PCA [14]. Wavelet packet transform was also tested on GPR data to remove the clutter, where the clutter threshold was determined based on higher-order-statistics [15]. Differentiating objects from clutter using linear prediction was proposed in [16], where the prediction was carried out in frequency domain to employ subband processing.

Most of the aforementioned techniques assume constant detector height, as variable sensor height has a deforming effect on the returning GPR signal. This assumption reduces the performance of the detectors in real life, where the ground may be highly wavy, or the operator of the detector may be unqualified. To the best of our knowledge, only successful study specifically carried out to make the detector invariant under different detector heights is [17], where quad-quad apparent conductivity from the quadrature components at two frequencies are computed. However, this study is only applicable on metal objects as frequency-domain electromagnetic induction sensors are used.

In this study, we adopt the one-sided linear prediction based method given in [16]. Our work focuses on the prediction of future signals in time domain rather than the frequency domain. We show that, by adaptively changing the samples which are used for predicting the future samples in a certain scheme, the signal corruption due to detector height change can be captured by the prediction algorithm and future samples can be generated accordingly. The residual error between the predicted signal and the returning signal can be regarded as the likelihood of the existence of a buried object in the inspected region. As the prediction algorithm is one-sided, only past samples are utilized, which makes the proposed method causal and applicable in real-time applications.

II. Methodology

The core motive of using linear prediction to detect the existence of buried objects is that, similarity between different clutter signatures is notably higher than the similarity between clutter signatures and object signatures. Hence, using the previous clutter signatures, we can successfully model the new clutter signatures, but not the object signatures. We further propose that, the signal corruption due to varying detector height can also be captured using the linear prediction algorithm.

GPR data consists of vectors, so called the A-scans, at each position which correspond to the signal return from different depth levels. Let $\mathbf{X}_i(k) = [\mathbf{x}_1(k), \mathbf{x}_2(k), ..., \mathbf{x}_L(k)]$ represent the ensemble of A-scans, where i is the index in the swinging direction of the detector, k is the depth index and L is the gathered number of A-scans. Each A-scan is represented as $\mathbf{x}_i(k) = [x_i(1), x_i(2), ..., x_i(M)]$, where M is the maximum

depth index. As a preprocessing step, each $\mathbf{x}_i(k)$ is filtered with a median filter, having a window size of 5. This filtering operation removes the impulsive noise inherent in the GPR A-scans. For simplicity of notation, we call the filtered A-scans again as $\mathbf{x}_i(k)$. Throughout this paper, each $\mathbf{x}_i(k)$ refers to the median filtered A-scan at the ith position.

The linear prediction model for the A-scans can be set forth as

$$\hat{\mathbf{x}}_i(k) = \sum_{m=1}^{p} a_m \mathbf{x}_{i-m}(k) \tag{1}$$

where $\hat{\mathbf{x}}_i(k)$ is the predicted A-scan, p is the prediction order and a_m is the mth prediction coefficient. The prediction error vector is the difference between the predicted vector and the real vector. Putting the previous samples in a matrix form, we can rewrite our linear prediction model as

$$\mathbf{x}_i(k) = \sum_{m=1}^{p} a_m \mathbf{x}_{i-m}(k) + \boldsymbol{\varepsilon}_i(k) = \bar{\mathbf{X}}_p(k)\mathbf{a}_i(m) + \boldsymbol{\varepsilon}_i(k) \tag{2}$$

where $\boldsymbol{\varepsilon}_i(k)$ is the prediction error vector, $\bar{\mathbf{X}}_p(k)$ is the matrix formed of the most recent p A-scans and $\mathbf{a}_i(m) = [a_1, a_2, ..., a_p]$ is the prediction coefficients vector for the current location. It was previously stated that, similarity between the A-scans gathered from clutter and a target is low. The measure of this similarity is the energy of the prediction error vector. A high error energy corresponds to a high deviation from the previous A-scans, which might be the indicator of a buried object. Squared prediction error is given as

$$\zeta_{\boldsymbol{\varepsilon}_i} = \boldsymbol{\varepsilon}_i(k)^T \boldsymbol{\varepsilon}_i(k) \tag{3}$$

where superscript T denotes the transpose operation. To compute the prediction error vector, we first need to calculate the prediction coefficients vector. For this purpose, we adopt the maximum likelihood approach. To estimate the prediction coefficients vector, we model the elements of the prediction error vector as independent and identically distributed zero-mean Gaussian random variables with variance σ^2. Under this assumption, the probability density function of $\mathbf{x}_i(k)$ in the absence of a buried object becomes an M-variate Gaussian distribution which can be written as the multiplication of M univariate Gaussians. Maximum likelihood estimate of $\mathbf{a}_i(m)$ is the vector maximizing this M-variate Gaussian probability density function. Exploiting the monotonic fashion of the natural logarithmic function, to maximize the M-variate Gaussian pdf, we can minimize the log likelihood given by

$$l(\mathbf{a}_i(m)) = (\mathbf{x}_i(k) - \bar{\mathbf{X}}_p(k)\mathbf{a}_i(m))^T (\mathbf{x}_i(k) - \bar{\mathbf{X}}_p(k)\mathbf{a}_i(m)). \tag{4}$$

Setting the derivative of $l(\mathbf{a}_i(m))$ with respect to $\mathbf{a}_i(m)$ to zero, we obtain the following maximum likelihood estimate for $\mathbf{a}_i(m)$:

$$\hat{\mathbf{a}}_i(m) = (\bar{\mathbf{X}}_p(k)^T \bar{\mathbf{X}}_p(k))^{-1} \bar{\mathbf{X}}_p(k)^T \mathbf{x}_i(k). \tag{5}$$

Using this estimate of prediction coefficients, the error energy becomes [16]:

$$\zeta_{\boldsymbol{\varepsilon}_i} = \mathbf{x}_i(k)^T \mathbf{x}_i(k) - \mathbf{x}_i(k)^T \bar{\mathbf{X}}_p(k) \hat{\mathbf{a}}_i(m). \tag{6}$$

The detection problem is now reduced to a simple binary hypothesis test, where $\zeta_{\boldsymbol{\varepsilon}_i}$ is compared to a threshold. In this context, $\zeta_{\boldsymbol{\varepsilon}_i}$ is our test statistic. If $\zeta_{\boldsymbol{\varepsilon}_i}$ exceeds the threshold, existence of a buried object is detected. Intuitively, the matrix of past samples $\bar{\mathbf{X}}_p(k)$ should not be updated if a buried object is sensed. However, we also want to update it in as many regions as possible to capture the signal distortion due to varying detector head height. With these requirements and limitations, we update $\bar{\mathbf{X}}_p(k)$ for each sample if the following criterion is satisfied:

$$\zeta_{\boldsymbol{\varepsilon}_i} - \frac{1}{i-1} \sum_{m=1}^{i-1} \zeta_{\boldsymbol{\varepsilon}_m} < \gamma. \tag{7}$$

Using this formulation, we detect the existence of a buried object if the deviation of $\zeta_{\boldsymbol{\varepsilon}_i}$ from the current mean of the squared error energies is high. The squared error energy in the existence of a buried object is much higher than that in the absence of it, hence the mean is dominated by this higher terms. This property of the algorithm allows us to also sense the object going out of the inspected range. In this condition, $\bar{\mathbf{X}}_p(k)$ is immediately updated. As this update is performed at every location without a target, effect of corruption of the signal due to slow variations in detector height is minimized by including the corrupted signals in the calculation of the maximum likelihood estimate of $\mathbf{a}_i(m)$.

Novel part of this work is the removal of the deteriorating effect of varying detector height in the buried object detection problem using GPR. We show that by adaptively changing $\bar{\mathbf{X}}_p(k)$ according to (7), the detection system can be made more robust. By setting γ appropriately, signal change due to varying detector height can be compensated, with a negligible suppression in the target signature.

III. Experimental Results

This section presents the detection results for the proposed adaptive linear prediction algorithm. The GPR data were collected at 3 different sites with different soil conditions. A total of 220 B-scans were collected, each of which consists of 256 A-scans. Disk-shaped mine equivalents including metallic and nonmetallic content were placed in each site. The size and content information of the objects is given in Table 1.

TABLE I
SIZE, CONTENT AND NUMBER OF BURIED OBJECTS

Object ID	Diameter	Height	Content	$\mathbf{N_{obj}}$
1	50 mm	30 mm	Metal	40
2	100 mm	30 mm	Metal	60
3	150 mm	30 mm	Metal	40
4	200 mm	30 mm	Metal	40
5	90 mm	45 mm	Plastic	40
TOTAL				**220**

The data were collected using a robotic arm, first and last points of which differ by 6 cm in distance to ground. This height difference models the imperfections that occur when the operator is swinging the handheld detector. This setup is exhibited in Fig. 1.

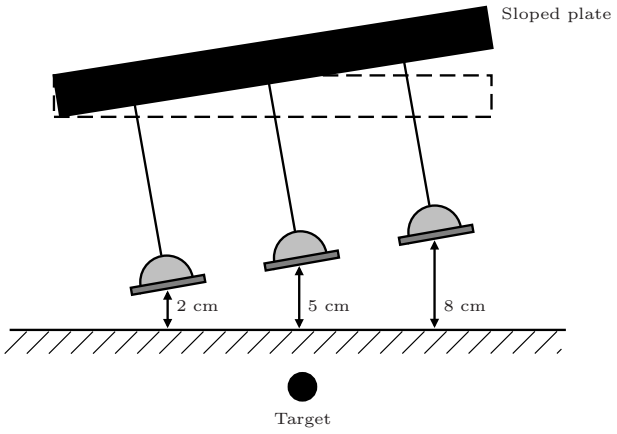

Fig. 1. Test setup

Existence of a buried object is decided whenever (7) is not satisfied, i.e., whenever the squared error energy is considerably different from the mean squared error energy. Although γ in (7) can be parameterized, we found out that setting γ to be 10^8 gave satisfactory results as well. The results presented in this section are calculated using this γ value. To comprehend the effect of adaptivity of the algorithm, a B-scan is first tested with nonadaptive linear prediction approach of [16]. The result is given in Fig. 2.

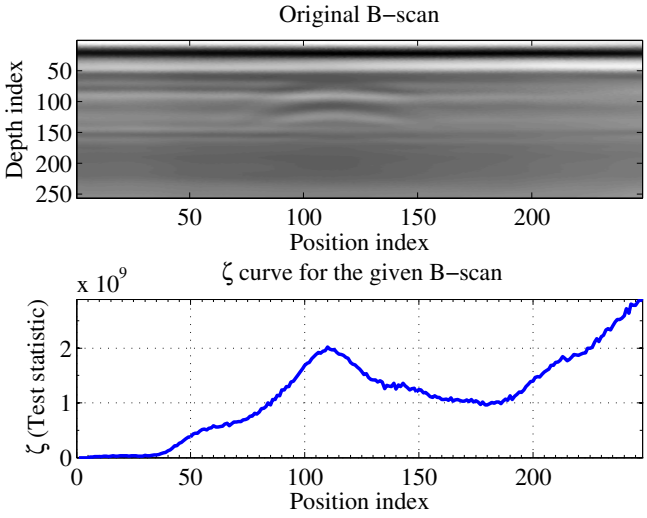

Fig. 2. A sample B-scan tested with nonadaptive linear prediction

In this scan, the buried object has a diameter of 5 cm and a height of 3 cm, and it is buried at 10 cm under the ground. It has completely metallic content. One can observe that, as the position index increases, intensity of the ground bounce increases in the B-scan. This shows that sensor is getting closer to the ground. The detector height change is 6 cm, which is very close to the height change in a handheld detector during swinging. As one can observe from Fig. 2, the test statistic fails to return to the idle state after passing over the buried object. The reason of this phenomenon is that, background update is stopped when the buried object is sensed. However, during the time that the detector passes over the object, an additional distortion due to detector height change is introduced. Using the clutter samples before the buried object, this new clutter samples cannot be represented, and a false alarm occurs. The same B-scan is tested with the proposed method for comparison. The result is given in Fig. 3.

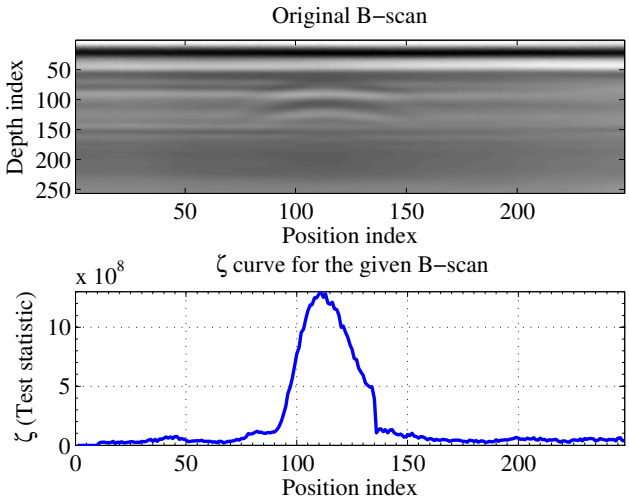

Fig. 3. Same B-scan tested with the proposed method

In both tests, the window size, which is given by p in the linear prediction model is selected as 10. Obviously, selecting a too small p causes the system to fail to model the clutter samples successfully. On the other hand, selecting a too large p allows the target signatures to be also modeled using the previous clutter samples. Hence, a moderate value of p must be found. In our tests, we found out that a p value between 5 and 20 suffices for our purposes. From Fig. 3, it is clear that, the false alarm region is eliminated. This flexibility is introduced by means of γ in (7). By setting γ carefully, one can set the extent to which the distortions due to height change will be suppressed. It should be noted that, when γ is chosen too large, the method boils down to nonadaptive linear prediction algorithm. On the other hand, setting a too small γ prevents the system to update the background signals. Hence, selection of γ requires great care.

As mentioned before, the proposed algorithm was tested on a real terrain and a total of 220 B-scans were gathered. Out of 220 objects, 216 of them were correctly detected, with 39 false alarms. Hence, detection rate is 98.2% and false alarm rate is 17.7%. Compared to conventional algorithms applied

to GPR data with varying detector height, false alarm rate is extremely reduced. A comparison of detection rates (P_d) and false alarm rates (FAR) of adaptive and nonadaptive linear prediction (LP) approaches are given in Table II.

TABLE II
COMPARISON OF ADAPTIVE AND NONADAPTIVE LP APPROACHES

	N_{obj}	P_d	FAR
Adaptive LP	220	98.2%	17.7%
Nonadaptive LP	220	99.5%	40.5%

In this table, N_{obj} stands for the total number of objects. One can see that, adaptive linear prediction provides a false alarm rate which is less than half of the false alarm rate of nonadaptive linear prediction method, with a negligible decrease in the probability of detection.

As other regressive approaches, the proposed method exploits past samples to decide on the next sample in normal operating conditions, i.e., in the absence of an underground anomaly. In the case of slowly varying clutter, this property of the algorithm provides noise immunity. However, when the clutter varies rapidly and unpredictably, it may degrade the detection performance considerably.

Future research will focus on the automated selection of γ according to soil conditions. Automating this process will provide a complete robustness to the detection system, thereby reducing the number of false alarms due to detector height variations of handheld detector systems.

IV. CONCLUSION

In this study, an adaptive linear prediction approach to buried object detection using GPR is proposed, with special emphasis on changes in detector height. In handheld GPR systems, the height changes are unavoidable and the detection algorithm must compensate for these changes. The proposed adaptive linear prediction method is shown to solve this problem to a considerable extent. We believe that this adaptivity must be an indispensable part of every buried object detection system, as there may be many imperfections in the returning GPR signal in real time applications.

REFERENCES

[1] L. B. Conyers and Tiffany Osburn, "GPR mapping to test anthropological hypotheses: a study from Comb Wash, Utah, American Southwest," in *11th Int. Conf. on Ground Penetrating Radar*, Columbus Ohio, USA, 2006, pp. 1-8.

[2] L. B. Conyers, "Ground-penetrating radar for landscape archaeology: method and applications," in *Seeing the Unseen*, S. Campana and S. Piro, Eds. Taylor and Francis Group, London, 2009, pp. 245-255.

[3] G. Leucci, S. Negri, "Use of ground penetrating radar to map subsurface archaeological features in an urban area," *J. Archaeol. Sci.*, vol. 33, pp. 502-512, Apr. 2006.

[4] J. R Butnor, M. L. Pruyn, D. C. Shaw, M. E. Harmon, A. N. Mucciardi and M. G. Ryan, "Detecting defects in conifers with ground penetrating radar: applications and challenges," *Forest Pathology*, vol. 39, pp. 309-322, Feb. 2009.

[5] T. Saarenketo and T. Scullion, "Road evaluation with ground penetrating radar," *J. Appl. Geophys.*, vol. 43, pp. 119-138, Mar. 2000.

[6] A. Neal, "Ground-penetrating radar and its use in sedimentology: principles, problems and progress," *Earth Sci. Rev.*, vol. 66, pp. 261-330, Jan. 2004.

[7] D. H. Koo and S. T. Ariaratnam, "Innovative method for assessment of underground sewer pipe condition," *Automat. Constr.*, vol. 15, pp. 479-488, July 2006.

[8] I. A. Lunta, S. S. Hubbardb and Y. Rubin, "Soil moisture content estimation using ground-penetrating radar reflection data," *J. Hydrol.*, vol. 307, pp. 254-269, 2005.

[9] D. J. Daniels, *Ground Penetrating Radar*, 2nd ed. IEE Radar, Sonar and Navigation Series 15, IEE, London, UK, 2004.

[10] P. D. Gader, B. N. Nelson, H. Frigui, G. Vaillette and J. M. Keller, "Fuzzy logic detection of landmines with ground penetrating radar," *Signal Process.*, vol. 80, pp. 1069-1084, June 2000.

[11] P. D. Gader, M. Mystkowski and Y. Zhao, "Landmine detection with ground penetrating radar using hidden Markov models," *IEEE T. Geosci. Remote*, vol. 39, pp. 1231-1244, June 2001.

[12] X. Xu, E. L. Miller, C. M. Rappaport and G. D. Sower, Statistical method to detect subsurface objects using array ground-penetrating radar data," *IEEE T. Geosci. Remote*, vol. 40, pp. 963-976, Apr. 2002.

[13] S. H. Yu, R. K. Mehra and T. R. Witten, "Automatic mine detection based on ground-penetrating radar," in *Proc. SPIE*, vol. 3710, pp. 961-972, 1999.

[14] P. P. Palit and S. Agarwal, "Independent component analysis for GPR based hand held mine detection," in *Proc. SPIE*, vol. 4742, p. 367-377, 2002.

[15] F. Abujarad, G. Nadim and A. Omar, "Wavelet Packets for GPR Detection of Non-Metallic Anti-Personnel Land Mines Based on Higher-Order-Statistic," in *3rd Int. Workshop on Advanced Ground Penetrating Radar*, Delft, The Netherlands, May 2005.

[16] K. C. Ho, P. D. Gader, "A linear prediction land mine detection algorithm for hand held ground penetrating radar," *IEEE T. Geosci. Remote*, vol. 40, pp. 1374-1384, June 2002.

[17] H. Huang, I. J. Won, "Electromagnetic detection of buried metallic objects using quad quad conductivity," *Geophysics*, vol. 69, pp. 1387, 2004.